



Thermodielectric Bistability in Dual Frequency Nematic Liquid Crystal

Y. Yin,¹ S. V. Shiyonovskii,^{1,2} and O. D. Lavrentovich^{1,2,*}

¹Chemical Physics Interdisciplinary Program, Kent State University, Kent, Ohio 44242, USA

²Liquid Crystal Institute, Kent State University, Kent, Ohio 44242, USA

(Received 7 December 2006; published 26 February 2007)

We report on a thermodielectric bistability in dual frequency nematic liquid crystals (LCs) caused by the anisotropic nature of dielectric heating and director reorientation in an electric field. The bistability is a result of the positive feedback loop: director reorientation \rightarrow anisotropic dielectric heating \rightarrow dielectric anisotropy \rightarrow director reorientation. We demonstrate both experimentally and theoretically that two states with different temperature and director orientation, namely, a cold planar state and a hot homeotropic state coexist in a LC cell for a certain frequency and amplitude range of the applied voltage.

DOI: 10.1103/PhysRevLett.98.097801

PACS numbers: 77.84.Nh, 42.79.Kr, 61.30.Dk, 77.22.Gm

The phenomenon that two stable states of a system coexist under the same external conditions is known as bistability. Bistability is found in atomic systems [1], gases [2], semiconductors [3], liquid crystals [4–8], biological cells [9], etc. Bistabilities in liquid crystals (LCs) are of special interest due to their applications in LC displays [5,7], spatial light modulators [4], optical information storage [6], etc. The bistabilities in LCs are caused by a balance of two different agents, such as an electric field \mathbf{E} that orients the LC director $\hat{\mathbf{n}}$ in the bulk, and surface anchoring that keeps the director aligned at the bounding substrates. In this work, we demonstrate a novel effect, in which the bistability originates from the electric field alone, through the balance of two different mechanisms of anisotropic coupling between \mathbf{E} and LC, namely, director reorientation and *anisotropic* dielectric heating.

When an electric field \mathbf{E} is applied to a LC, it exerts a torque on the director $\hat{\mathbf{n}}$ that depends on dielectric anisotropy $\Delta\epsilon = \text{Re}(\epsilon_{\parallel} - \epsilon_{\perp})$, where ϵ_{\parallel} and ϵ_{\perp} are the dielectric permittivity components corresponding to $\hat{\mathbf{n}} \parallel \mathbf{E}$ and $\hat{\mathbf{n}} \perp \mathbf{E}$, respectively. For LCs with $\Delta\epsilon > 0$, $\hat{\mathbf{n}}$ reorients parallel to \mathbf{E} ; if $\Delta\epsilon < 0$, then $\hat{\mathbf{n}} \perp \mathbf{E}$. In the so-called dual frequency nematic (DFN) LC, $\Delta\epsilon$ changes sign from $\Delta\epsilon > 0$ at $f < f_c$ to $\Delta\epsilon < 0$ at $f > f_c$ as the function of the applied field frequency f . The crossover frequency f_c corresponds to the dispersion region of the *parallel* component of dielectric permittivity ϵ_{\parallel} ; f_c is a strong monotonically increasing function of temperature. In addition to the dielectric reorienting torque [10], the electric field causes heating of the LC, especially in the dispersion region. As the result, the heating is essentially an *anisotropic effect*: the temperature increase is maximum when $\hat{\mathbf{n}} \parallel \mathbf{E}$ and minimum when $\hat{\mathbf{n}} \perp \mathbf{E}$. The two mechanisms of coupling between \mathbf{E} and LC thus set up a possibility of a bistability of two states that can coexist at a given \mathbf{E} : a cold planar (CP) state and a hot homeotropic (HH) state. The idea can be explained by the following *gedanken* experiment. One starts an experiment with a DFN sandwiched between two flat electrodes. A modest electric voltage U is applied at $f > f_c$ (so that $\Delta\epsilon < 0$) to stabilize the CP state,

$\hat{\mathbf{n}} \perp \mathbf{E}$. An increasing U would increase the LC temperature T , up to the point T_c where the inversion frequency $f_c(T)$ exceeds f and $\Delta\epsilon$ becomes positive. With $\Delta\epsilon > 0$, the director reorients into the HH state, $\hat{\mathbf{n}} \parallel \mathbf{E}$. The voltage $U_{\text{CP} \rightarrow \text{HH}}$ of the CP \rightarrow HH transition is relatively high because in the CP state the dielectric heating is minimum. In the HH state, however, the dielectric heating is more efficient than in the CP state. The threshold $U_{\text{HH} \rightarrow \text{CP}}$ of the reverse HH \rightarrow CP transition, caused by decreasing U to reach T_c from above in the HH state, should be lower than $U_{\text{CP} \rightarrow \text{HH}}$. Therefore, because of the anisotropic nature of both dielectric heating and dielectric reorientation of the director, one would expect a bistability, i.e., a coexistence of the CP and HH states in the certain range of voltages, $U_{\text{HH} \rightarrow \text{CP}} < U < U_{\text{CP} \rightarrow \text{HH}}$. Below, we first demonstrate the phenomenon experimentally and then describe it with a quantitative model that, in addition to the consideration of the bulk dielectric reorientation and heating, takes into account the surface anchoring effects at the bounding plates (which hinders the occurrence of bistability rather than causes it, as in other known cases [4–8]).

We used a DFN mixture MLC2048 (EM Industries). The real (ϵ'_{\parallel} , ϵ'_{\perp}) and imaginary (ϵ''_{\parallel} , ϵ''_{\perp}) components of the dielectric permittivity tensor of MLC2048 were measured using the Impedance/Gain-Phase analyzer SI-1260 (Schlumberger Inc.) in the range $f = (1-500)$ kHz at $T_0 = 24.0^\circ\text{C}$, Fig. 1. The sign reversal of $\Delta\epsilon$ is caused by the dispersion of ϵ_{\parallel} and the maximum value of ϵ''_{\parallel} is reached at f_c .

We filled MLC2048 into a cell of a thickness $d = 11 \mu\text{m}$. The indium tin oxide electrodes at the inner surfaces of the cell's bounding glass plates were coated with a polyimide layer SE-7511 (Nissan Chemicals) to set $\hat{\mathbf{n}}$ perpendicular to the bounding plates; this homeotropic alignment allows us to identify unambiguously the HH state as a “black” state in observations with crossed polarizers. The cell was placed inside a LTS-350 hotstage (Linkam) permitting temperature stabilization at $T_0 = 24.00 \pm 0.01^\circ\text{C}$. To improve the uniformity of the thermal

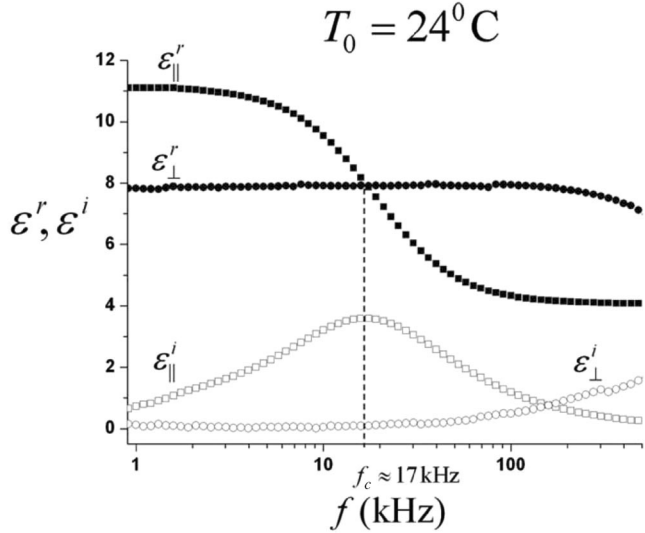


FIG. 1. The measured real (ϵ^r) and imaginary (ϵ^i) parts of the dielectric permittivity tensor of MLC2048 in the frequency range 1 to 500 kHz at 24 °C. The error bars are smaller than the size of the data points.

environment around the cell, we created an air gap between the cell and the hot stage, by separating them with two wood rods of 0.5 mm diameter. We measured the temperature T_g , at the outer surface of the glass plate bounding the LC, by an attached thermocouple. According to our previous studies [11], (a) the heat flux Q_{out} at the interface between the cell and the surrounding medium obeys the Newton's cooling law; i.e., $Q_{\text{out}} = k(T_g - T_0)$, where k is the heat transfer coefficient of the glass-air interface, and (b) the temperature gradient across the LC layer is small, less than 0.01 °C. Thus the average temperature T of the LC layer at the thermal equilibrium is related to T_g as [12],

$$T - T_0 = (1 + \text{Bi})(T_g - T_0), \quad (1)$$

where $\text{Bi} = kL/G$ is the Biot number, $L = 1.1$ mm and $G = 1 \text{ W m}^{-1} \text{ K}^{-1}$ are the thickness and thermal conductivity [13] of the glass plate, respectively. With the typical $k = 10\text{--}50 \text{ W m}^{-2} \text{ K}^{-1}$ [14], Bi is very small, 0.01–0.05, and thus, according to Eq. (1), T_g yields a good quantitative measure of T .

We applied a harmonic voltage $\tilde{U} = \sqrt{2}U \cos 2\pi ft$ with varying rms voltage U . We have chosen $f = 20$ kHz, because T_c for this frequency is 26 °C, i.e., slightly larger than T_0 , Fig. 2. The rms voltage was changed in steps of 0.2 V with 400 s equilibration time; the latter is enough to achieve an equilibrium temperature within 0.01 °C [11], the accuracy of the temperature control. The state of the cell placed between two crossed polarizers of a microscope was monitored through the textural (Fig. 3) and light transmittance changes (Fig. 4); the polarizers were aligned to maximize the transmittance in the CP state.

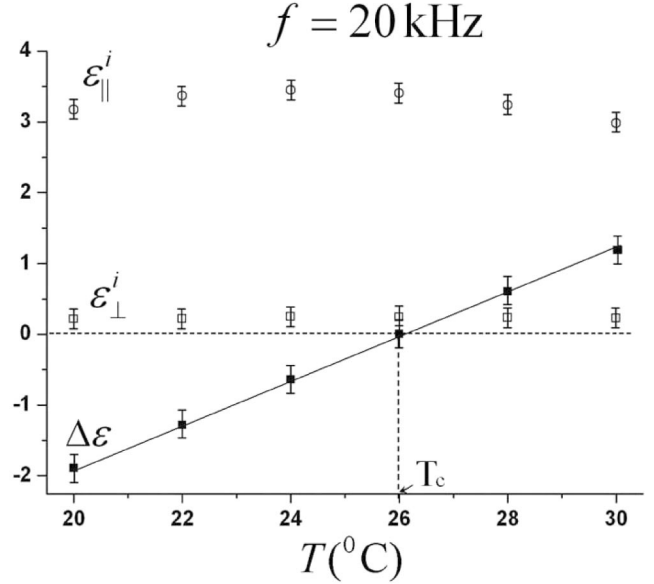


FIG. 2. The dielectric properties of MLC2048 at 20 kHz as a function of temperature. The straight line corresponds to the linear fit for $\Delta\epsilon(T)$, Eq. (5).

The initial homeotropic state transforms into a state with $\hat{\mathbf{n}}$ tilted away from \mathbf{E} when the applied voltage exceeds the Fredericks threshold $U_F^0 = \pi(K_{33}/\epsilon_0|\Delta\epsilon(T_0)|)^{1/2} \approx 6$ V; this state is an analog of the CP state in the gedanken experiment, the only difference is that $\hat{\mathbf{n}}$ is not strictly parallel to the bounding plates (because of the surface anchoring at the bounding plates). We will continue to label this “cold tilted” state as the CP state. The CP state appears as a bright texture under the crossed polarizers (insets 1 and 2 in Fig. 3); light transmission is high, Fig. 4. Small increments of voltage lead to small increments of the

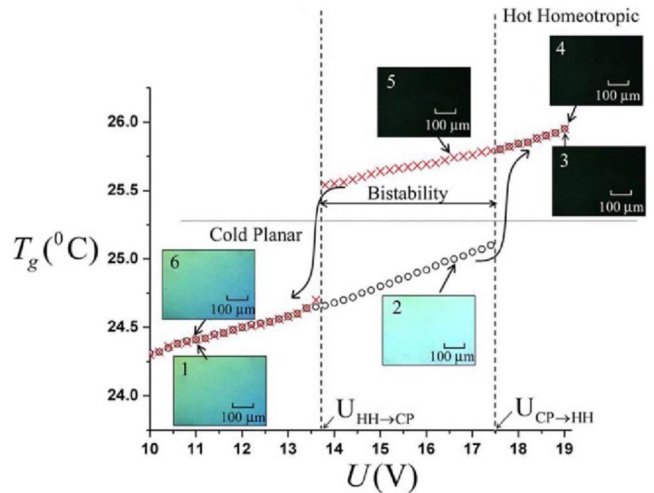


FIG. 3 (color online). The thermoelectric bistability: the measured temperature T_g vs increasing (circles) and decreasing (crosses) applied voltage. The insets exhibit images in a polarizing microscope with crossed polarizers.

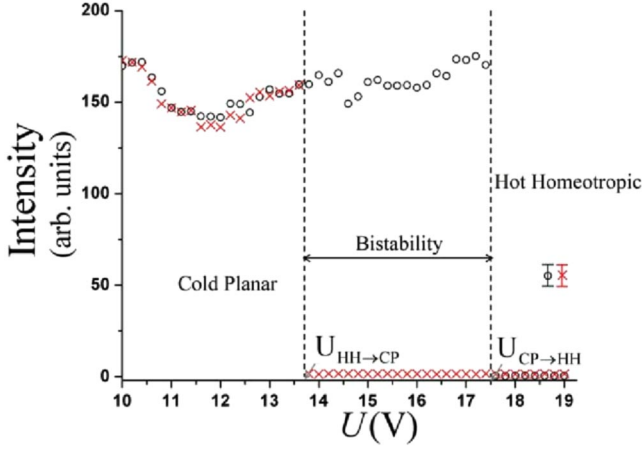


FIG. 4 (color online). The transmitted light intensity vs increasing (circles) and decreasing (crosses) applied voltage. The error bars correspond to the intensity data in the CP state; in the HH state the error bars are smaller than the cross size.

measured temperature T_g . However, at some voltage $U_{CP \rightarrow HH}$, the CP structure transforms abruptly into a dark HH texture (inset 3 in Figs. 3 and 4) with a substantial increase of T_g . Further voltage increases produce relatively small temperature increases, Fig. 3. In the reverse process of lowering the voltage, the HH state persists until the voltage is reduced to $U_{HH \rightarrow CP}$, well below $U_{CP \rightarrow HH}$ (by 3.8 V, Figs. 3 and 4). The cell becomes transparent again, as the director tilts away from the homeotropic orientation, inset 6 in Fig. 3. The experiment thus clearly shows the bistability regime in the range $U_{HH \rightarrow CP} < U < U_{CP \rightarrow HH}$.

The model of the phenomenon is based on the self-consistent consideration of the temperature and director fields in a cell with surface anchoring. The harmonic voltage $\tilde{U} = \sqrt{2}U \cos 2\pi ft$ creates an electric field $\mathbf{E} = \tilde{U} \hat{\mathbf{z}}/d$ that is assumed to be homogeneous within the LC as $\Delta\epsilon$ is small for the frequency range of interest.

The dielectric heating power density P of the LC layer is [15]

$$P = f \int_0^{1/f} \mathbf{E} \cdot \frac{\partial \mathbf{D}}{\partial t} dt = \frac{2\pi f \epsilon_0 \epsilon_{zz}^i U^2}{d^2}, \quad (2)$$

where D is the electric displacement, $\epsilon_{zz}^i = \frac{1}{d} \times \int_0^d [\epsilon_{\perp}^i \sin^2 \theta(z) + \epsilon_{\parallel}^i \cos^2 \theta(z)] dz$ is the imaginary part of the average dielectric permittivity, and θ is the angle between the director $\hat{\mathbf{n}}$ and the normal $\hat{\mathbf{z}}$ of the bounding plates.

The thermal balance between the heat generation and dissipation $Q_{in} = Pd/2 = Q_{out}$, determines the equilibrium LC temperature T :

$$T = T_0 + \frac{\pi(1 + \text{Bi})f \epsilon_0 \epsilon_{zz}^i U^2}{kd}. \quad (3)$$

The characteristic time of the temperature dynamics is $\tau_T = c_p \rho L^2 / G q_1^2 \approx 30$ s, where c_p is the heat capacity of

the glass plate, ρ is the glass density, and $q_1 \approx \text{Bi}^{1/2}$ is the smallest positive root of the equation $q_1 \tan q_1 = \text{Bi}$ [11]. Because τ_T is much larger than the director reorientation time $\tau \sim 10^{-2}$ s, the director configuration can be found as an equilibrium state of a cell with elastic and dielectric properties that correspond to the current temperature.

Let us start with situation when the director orientation at the bounding plates is not fixed by surface anchoring, to show the essence of the effect and the importance of dielectric heating anisotropy. In the anchoring-free case, the equilibrium state is either strictly homeotropic, $\hat{\mathbf{n}} \parallel \mathbf{E}$, when $\Delta\epsilon(T) > 0$, or strictly planar, $\hat{\mathbf{n}} \perp \mathbf{E}$, when $\Delta\epsilon(T) < 0$. Thus, both transitions should start at $T = T_c$ and the bistability range $U_{HH \rightarrow CP} < U < U_{CP \rightarrow HH}$ should be determined by anisotropy of the dielectric heating, as $U_{HH \rightarrow CP} = U_0 / (\epsilon_{\parallel}^i)^{1/2}$ and $U_{CP \rightarrow HH} = U_0 / (\epsilon_{\perp}^i)^{1/2}$, where $U_0 = [(T_c - T_0)kd / (\pi(1 + \text{Bi})f \epsilon_0)]^{1/2}$. Note that the anisotropy of dielectric heating must be positive, i.e., $\epsilon_{\parallel}^i > \epsilon_{\perp}^i$, for the effect to take place.

In a cell with $\hat{\mathbf{n}}$ fixed by surface anchoring at the plates, the equilibrium field-induced distortion of $\hat{\mathbf{n}} = \hat{\mathbf{n}}(z)$ has a well-known analytical solution [16]. For small $\epsilon_{\parallel}^i - \epsilon_{\perp}^i < 0$, and for one constant approximation of the LC elasticity, this solution relates ϵ_{zz}^i , U and the maximum angle θ_m in the middle of the LC layer:

$$U = 2 \left(\frac{K}{\epsilon_0 |\Delta\epsilon(T)|} \right)^{1/2} \mathbf{K}(\sin^2 \theta_m), \quad (4)$$

$$\epsilon_{zz}^i = \epsilon_{\perp}^i + (\epsilon_{\parallel}^i - \epsilon_{\perp}^i) \frac{\mathbf{E}(\sin^2 \theta_m)}{\mathbf{K}(\sin^2 \theta_m)},$$

where K is elastic constant of the LC, $\mathbf{K}(\sin^2 \theta_m)$ and $\mathbf{E}(\sin^2 \theta_m)$ are the complete elliptic integrals of the first and second kind, respectively [17].

To describe the bistability, in addition to Eqs. (3) and (4), one needs to specify the dependence $\Delta\epsilon(T)$; Fig. 2 shows that it follows a linear behavior,

$$\Delta\epsilon(T) = a(T_C - T), \quad (5)$$

where $a = 0.316 \text{ } ^\circ\text{C}^{-1}$, $T_C = 26.0 \text{ } ^\circ\text{C}$.

Equations (3)–(5) allow us to find an analytical solution describing $T(U)$ and $\theta_m(U)$, Fig. 5. The bistability is controlled by the anisotropy of dielectric heating, $\Delta\epsilon^i = \epsilon_{\parallel}^i - \epsilon_{\perp}^i$. In Fig. 5, we fix $\epsilon_{\parallel}^i = 3.5$ (which is characteristic of MLC2048, Fig. 2) and analyze the scenarios for three different ϵ_{\perp}^i 's, corresponding to $\Delta\epsilon^i = 0$ (curve 1), $\Delta\epsilon^i = 0.93$ (curve 2), and $\Delta\epsilon^i = 3.1$ (curve 3). Curve 1 describes the “usual” monostable sequence characteristic of zero heating anisotropy. The LC layer, originally in the homeotropic state, experiences a regular Frederiks transition into a tilted CP state $\theta_m > 0$ above some modest threshold U_F , Fig. 5, curve 1. A further voltage increase leads to an increase of θ_m but it also increases T . Because of the latter, $\Delta\epsilon$ decreases to zero and at some U_{RF} , the cell experiences a reverse Frederiks (RF) transition, back to $\theta_m = 0$.

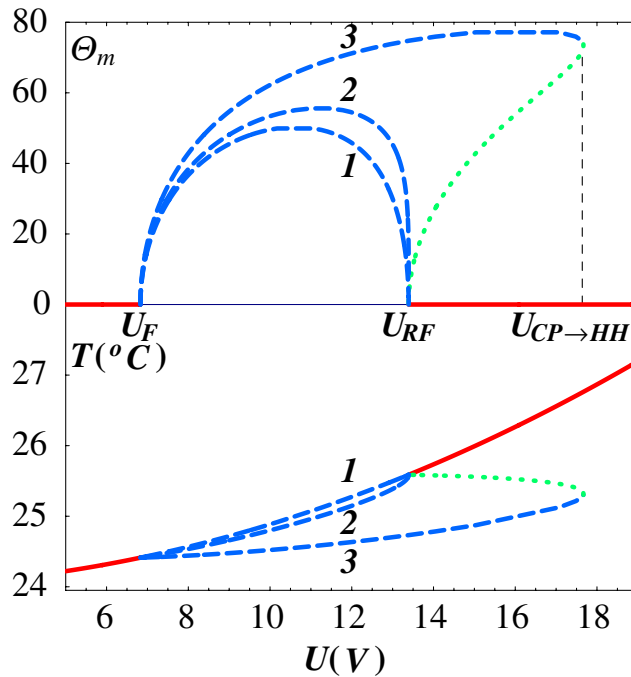


FIG. 5 (color online). The simulation of thermodielectric bistability exhibited in $\theta_m(U)$ and $T(U)$ for CP (dashed curves), HH (solid curves), and unstable (dotted curves) states in a homeotropic cell with different ϵ_{\perp}^i : (1) 0.45, (2) 2.57, (3) 3.2. The other parameters correspond to MLC2048 and the experiment presented above. The heat transfer coefficient of the air-glass interface $k = 20 \text{ W m}^{-2} \text{ K}^{-1}$ is chosen to make curve 3 close to the experimental data.

Decreasing U would result in the reverse sequence of transitions without any hysteresis. The scenario changes completely if the heating anisotropy is positive and large enough, curve 3. The original state $\theta_m = 0$ is converted into the CP state $\theta_m > 0$ at the same U_F , but because the heat production in this state is relatively low ($\epsilon_{\perp}^i \ll \epsilon_{\parallel}^i$), the dielectric anisotropy $\Delta\epsilon$ remains positive and the CP state is retained even for voltages above U_{RF} ; it transforms abruptly into the HH state only at some $U_{CP \rightarrow HH} > U_{RF}$. Upon reduction of the voltage, the HH state returns into the CP state at $U_{HH \rightarrow CP} = U_{RF}$, hence a bistability. Finally, curve 2 is a critical regime separating the monostable and bistable behaviors.

The model (curve 3) describes the experimental data very closely, as evident from the predicted voltage and temperature range of the bistability; compare Figs. 3 and 5. Clearly, some model simplifications, such as one-constant elasticity, the exact value of k , and cell imperfections, such as director distortions around the spacers or finite electric conductivity of the cell, might cause quantitative discrepancies, but the overall agreement is good.

To conclude, we observed and interpreted the thermodielectric bistability that is caused by a competition of dielectric heating and director reorientation of the LC in an electric field. For the effect to occur, the dielectric heating should be anisotropic (i.e., dependent on the director orientation with respect to the applied electric field), a feature that has not been appreciated much in the literature so far. The thermodielectric bistability might be of practical importance, because (a) the optical contrast between the HH and CP states is extremely sharp, as the director reorients substantially, from $\theta_m \approx 0^\circ$ to $\theta_m \approx 70^\circ$ at the HH-CP transition, Fig. 5, and (b) the states can be switched between with a very low power when the frequency of the applied voltage is only slightly above the crossover frequency.

The work was supported by DOE Grant No. DE-FG02-06ER 46331.

*Electronic address: odl@lci.kent.edu

- [1] M. P. Hehlen, H. U. Gudel, Q. Shu, J. Rai, S. Rai, and S. C. Rand, *Phys. Rev. Lett.* **73**, 1103 (1994).
- [2] H. M. Gibbs, S. L. McCall, and T. N. C. Venkatesan, *Phys. Rev. Lett.* **36**, 1135 (1976).
- [3] D. A. B. Miller, S. D. Smith, and A. Johnston, *Appl. Phys. Lett.* **35**, 658 (1979).
- [4] N. A. Clark and S. T. Lagerwall, *Appl. Phys. Lett.* **36**, 899 (1980).
- [5] D. Yang, J. L. West, L. C. Chien, and J. W. Doane, *J. Appl. Phys.* **76**, 1331 (1994).
- [6] U. Bortolozzo and S. Residori, *Phys. Rev. Lett.* **96**, 037801 (2006).
- [7] O. O. Ramdane, P. Auroy, S. Forget, E. Raspaud, P. Martinot-Lagarde, and I. Dozov, *Phys. Rev. Lett.* **84**, 3871 (2000).
- [8] B. Wen and C. Rosenblatt, *Phys. Rev. Lett.* **89**, 195505 (2002).
- [9] J. E. Ferrell, *Curr. Opin. Chem. Biol.* **14**, 140 (2002).
- [10] Y. Yin, S. V. Shiyonovskii, A. B. Golovin, and O. D. Lavrentovich, *Phys. Rev. Lett.* **95**, 087801 (2005).
- [11] Y. Yin, S. V. Shiyonovskii, and O. D. Lavrentovich, *J. Appl. Phys.* **100**, 024906 (2006).
- [12] See, for example, A. V. Luikov, *Analytical Heat Diffusion Theory* (Academic, New York, 1968).
- [13] H. P. R. Frederikse and D. R. Lide, *Handbook of Chemistry and Physics* (CRC, Boca Raton, Florida, 1994).
- [14] R. H. Turner and Y. A. Cengel, *Fundamentals Of Thermal-fluid Sciences* (McGraw-Hill, New York, 2004), 2nd ed.
- [15] J. D. Jackson, *Classical Electrodynamics* (Wiley, New York, 1962).
- [16] H. J. Deuling, *Mol. Cryst. Liq. Cryst.* **19**, 123 (1972).
- [17] M. Abramowitz and I. A. Stegun, *Handbook of Mathematical Functions* (Dover, New York, 1970).